Eur. Phys. J. D **16**, 81–85 (2001)

THE EUROPEAN PHYSICAL JOURNAL D

EDP Sciences
© Società Italiana di Fisica
Springer-Verlag 2001

Trianionic gold clusters

C. Yannouleas[1,a], U. Landman[1], A. Herlert[2], and L. Schweikhard[2]

[1] School of Physics, Georgia Institute of Technology, Atlanta, GA 30332-0430, USA
[2] Institut für Physik, Johannes Gutenberg-Universität, D-55099 Mainz, Germany

Received 9 January 2001

Abstract. Using Penning-trap experiments and a shell-correction method incorporating ellipsoidal shape deformations, we investigate the formation and stability patterns of trianionic gold clusters. Theory and experiment are in remarkable agreement concerning appearance sizes and electronic shell effects. In contrast to multiply cationic clusters, decay of the trianionic gold clusters occurs primarily *via* electron autodetachment and tunneling through a Coulomb barrier, rather than *via* fission.

PACS. 36.40.Wa Charged clusters – 36.40.Qv Stability and fragmentation of clusters – 36.40.Cg Electronic and magnetic properties of clusters

1 Introduction

While electrical charging of macroscopic metal capacitors has been a familiar subject since the earliest days of electricity [1], only recently the charging of nanostructures emerged as an active research field in diverse areas of condensed-matter, molecular, and cluster physics. The systems involved include semiconductor quantum dots [2], as well as various gas-phase microsystems such as carbon clusters and fullerenes [3,4], large organic molecules [5] and metal clusters [6–10].

Although observations [3] of the gas-phase carbon clusters and fullerenes were reported in 1990-1991, the observation of gas-phase multiply anionic metal clusters continued to remain until recently an outstanding experimental challenge. Indeed theoretical studies had been performed several years ago [11(a)], but only recently the first dianionic metal clusters Au_N^{2-} were observed [12]. Soon thereafter additional observations of dianionic and trianionic gas-phase metal clusters for several other materials were reported [13–16].

The case of dianionic gold and silver clusters has been discussed in detail elsewhere, both experimentally [13,16] and theoretically [11(b)]. In the following, we will focus on studying the generation and stability of *triply anionic* gas-phase metal clusters, in particular of Au_N^{3-}. The theoretical conclusions concerning the stability and decay channels of Au_N^{3-}, as well as their appearance sizes, n_a^{3-}, are fully supported by experimental observations of the production yields [17].

Macroscopic metal capacitors may be charged at will, but for gas-phase metal clusters there are intrinsic limits dependent on the material and the size of the cluster. These limits are due to instabilities arising from the confinement of excess charges to a small volume of microscopic dimensions. Of particular interest is the fact that triply anionic gold clusters behave remarkably differently than their cationic counterparts [18]: they dissociate *via* a different decay channel, *i.e.*, electron autodetachment through a repulsive Coulomb barrier (CB) [19], instead of fragmenting *via* fission. Although they differ in their decay channels, the triply charged metal-cluster anions exhibit shape-dependent electronic shell effects [8,9], in analogy with the neutral and cationic species.

2 Theory

Theoretically, two classes of decay channels need to be considered for the appearance sizes of the Au_N^{3-} clusters: (i) binary and ternary fission channels,

$$Au_N^{3-} \rightarrow Au_P^{2-} + Au_{N-P}^{-}, \quad (1)$$

$$Au_N^{3-} \rightarrow Au_P^{-} + Au_Q^{-} + Au_{N-P-Q}^{-}, \quad (2)$$

which have well known analogs in the case of multiply cationic clusters [6–8] and atomic nuclei [20], and (ii) electron autodetachment *via* tunneling through a repulsive Coulombic barrier [11],

$$Au_N^{3-} \rightarrow Au_N^{2-} + e, \quad (3)$$

in analogy to proton and alpha decay in atomic nuclei [20,21].

For the theoretical analysis of the energetics of these channels, we use a finite-temperature semi-empirical shell-correction method (FT-SCM), which has been previously used successfully to describe the properties of neutral and

[a] e-mail: constantine.yannouleas@physics.gatech.edu

cationic metal clusters [8,9]. This FT-SCM, developed by two of the authors, incorporates three important aspects, namely, triaxial deformations, entropy of the electrons, and thermal effects originating from shape fluctuations.

Since the number of delocalized valence electrons is fixed for a given cluster, M_N^{x-}, we need to use [22,23] the *canonical* ensemble in calculating their thermodynamical properties. For determining the free energy, $F(\beta, N, x)$ ($\beta = 1/T$), which incorporates the electronic entropy, we separate it, in analogy with the zero-temperature limit [9(a)], into a smooth, liquid-drop-model part, $\widetilde{F}_{LDM}$, and a Strutinsky-type [24] shell-correction term, ΔF_{sh}. The shell correction term is specified as the difference $\Delta F_{sh} = F_{sp} - \widetilde{F}_{sp}$, where F_{sp} is the canonical free energy of the valence electrons viewed as independent single particles in their effective mean-field potential. For calculating the canonical F_{sp}, we adopt a number-projection method [25], according to which

$$F_{sp} = -\frac{1}{\beta} \ln \left\{ \int_0^{2\pi} \frac{d\phi}{2\pi} Z_{GC}(\beta, \beta\mu + i\phi) e^{-(\beta\mu + i\phi)N_e} \right\}, \tag{4}$$

where N_e is the number of electrons and μ is the chemical potential of the equivalent grand-canonical ensemble. The grand-canonical partition function, Z_{GC}, is given by

$$Z_{GC}(\beta, \beta\mu) = \prod_i (1 + e^{-\beta(\varepsilon_i - \mu)}), \tag{5}$$

where ε_i are the single-particle levels of the modified Nilsson Hamiltonian pertaining to triaxial shapes [9(a)]. The temperature dependent average $\widetilde{F}_{sp}$ [26] is specified using the same expressions as for F_{sp}, but with a set of smooth levels defined as $\widetilde{\varepsilon}_i = \widetilde{E}_{sp}^{osc}(i) - \widetilde{E}_{sp}^{osc}(i-1)$, where $\widetilde{E}_{sp}^{osc}(N_e)$ is the zero-temperature Strutinsky average of the single-particle spectrum of an anisotropic, triaxial oscillator (see section II.C. of Ref. [9(a)]).

The LDM term $\widetilde{F}_{LDM}$ consists of three contributions: a volume, a surface, and a curvature term. Since volume conservation during deformation is assumed, we need not consider the temperature dependence of the corresponding term when calculating observables, such as EA's or IP's, associated with processes which do not change the total number of atoms, N. The experimental temperature dependence of the surface tension, $\sigma(T) = c_0 - c_1(T - T_{mp})$, is taken from standard tables [27] (T_{mp} are melting-point temperatures [28]), but normalized to yield the $\sigma(T = 0)$ value used in our earlier calculations [9(a)]. Since no experimental information is available regarding the curvature coefficient, A_c, we assume the same relative temperature dependence as for $\sigma(T)$ normalized to the $T = 0$ value used earlier [9(a)]. Finally, the expansion of the Wigner-Seitz radius due to the temperature is determined according to the coefficient of linear thermal expansion [28]. With these modifications, the remaining steps in the calculation of $\widetilde{F}_{LDM}$ follow closely section II.A. of Ref. [9(a)].

According to the general theory of thermal fluctuating phenomena [29], the triaxial shapes of the clusters, specified by the β_H and γ_H Hill-Wheeler parameters [30], will explore [31] the free-energy surface, $F(\beta, N, x; \beta_H, \gamma_H)$, with a probability,

$$P(\beta_H, \gamma_H) = \mathcal{Z}^{-1} \exp[-\beta F(\beta, N, x; \beta_H, \gamma_H)], \tag{6}$$

the quantity $\mathcal{Z}$ being the classical Boltzmann-type partition function,

$$\mathcal{Z} = \int d\tau \exp[-\beta F(\beta, N, x; \beta_H, \gamma_H)], \tag{7}$$

and $d\tau = \beta_H^4 |\sin(3\gamma_H)| d\beta_H d\gamma_H$ the proper volume element [32]. Thus, finally, the free energy, $\langle F(\beta, N, x) \rangle$, averaged over the shape fluctuations can be written as

$$\langle F(\beta, N, x) \rangle = \int d\tau F(\beta, N, x; \beta_H, \gamma_H) P(\beta_H, \gamma_H). \tag{8}$$

The finite-temperature multiple electron affinities of a cluster of N atoms of valence v (we take $v = 1$ for Au) are defined as

$$A_x(N, \beta) = F(\beta, vN, vN + x - 1) - F(\beta, vN, vN + x), \tag{9}$$

where F is the free energy, $\beta = 1/k_B T$, and $x \geq 1$ is the number of excess electrons in the cluster (*e.g.*, the first, second, and third electron affinities correspond to $x = 1$, $x = 2$, and $x = 3$ respectively). The smooth contribution $\widetilde{A}_x(N, \beta)$ to the full multiple electron affinities $A_x(N, \beta)$ can be approximated by the LDM expression [11(a)],

$$\widetilde{A}_x = \widetilde{A}_1 - \frac{(x-1)e^2}{R(N) + \delta_0} = W - \frac{(x - 1 + \gamma)e^2}{R(N) + \delta_0}, \tag{10}$$

where $R(N) = r_s N^{1/3}$ is the radius of the positive background (r_s is the Wigner-Seitz radius which depends weakly on T due to volume dilation), $\gamma = 5/8$, δ_0 is an electron spillout parameter. For simplicity, the work function W is assumed to be temperature independent [we take W(Au)= 5.31 eV].

3 Experiment

Trianionic gold clusters have been produced and observed by use of a Penning trap system devoted to metal cluster research [33]. The present procedure is the same as for the case of dianionic silver clusters as described in detail elsewhere [16]: Singly charged clusters Au_N^- from a Smalley-type ion source [34] are transferred by ion-optical elements through differential-pumping stages and captured in flight in a Penning trap [35]. This device acts as a wall-less container for ions by the combination of a strong magnetic field and an electric trapping potential along the magnetic field lines [36].

After size selection the clusters of interest are subjected to the presence of simultaneously stored electrons which are created by electron-impact ionization of argon atoms inside the trap volume. The clusters are observed to

pick up one or two further electrons. This reaction is analyzed by time-of-flight mass spectrometry after axial ejection of the cluster ions. A typical experimental sequence lasts a few seconds and a few tens of ions are observed in each experimental cycle by single-ion counting. The signal intensity of several hundred sequences is summed to increase the statistical significance of the data.

The electron pickup is influenced by many experimental conditions. However, if the parameters are kept constant the relative conversion yields are found to give valuable information on the clusters' properties. In particular, it has been suggested [11(b), 12, 13] that the resulting experimental yield patterns reflect the clusters' multiple electron affinities. The case of Au_N^{3-} considered here and that of Ag_N^{2-} [16] show this to be a general feature applicable to any excess charge and cluster species.

4 Results

In Fig. 1(a), we display the SCM theoretical results [37,38] for the second, A_2, and third, A_3, electron affinities of Au_N clusters in the size range $50 \leq N \leq 70$. Multiply anionic clusters M_N^{x-} with $A_x < 0$ are unstable [11] against electron emission *via* tunneling through a CB. In the case of doubly anionic gold clusters, all sizes in the aforementioned range are stable, *i.e.*, they have $A_2 > 0$ [see upper curve in Fig. 1(a)]. In contrast, for the gold-cluster trianions, those with $N \leq 53$ and $56 \leq N \leq 62$ have $A_3 < 0$. Thus, the appearance size for Au_N^{3-} is $n_a^{3-} \approx 54$. Apparently, the major shell closure at 58 electrons (corresponding to the Au_{56}^{2-} parent of the triply charged Au_{56}^{3-} cluster) creates an island of stability (the clusters with $N = 54$ and 55 have $A_3 > 0$) preceding the main stability branch (with $N \geq 63$).

Figure 1(b) shows the observed relative abundances for Au_N^{2-} and Au_N^{3-} in the same size range. Day-to-day variations of the experimental parameters lead to values that differ somewhat more than expected from the statistical uncertainties of the individual measurements. (In general the variations of the trianion values correspond to those of the dianions.)

While dianionic gold clusters are observed for all sizes under investigation ($50 \leq N \leq 70$) as expected [11(b), 13] [$n_a^{2-}(\mathrm{Au}) = 12$], there is no obvious structure in the dianion yield as a function of cluster size. This is in contrast to earlier observations of dianions at the threshold size [13]. The trianion yields are two to three orders of magnitude smaller than the ones of the dianions, reflecting the difference in the magnitudes of the associated multiple electron affinities [see Fig. 1(a)]. In addition, however, the trianions show a yield maximum at about $N = 55$ and a minimum around $N = 59$ before the yield rises again and levels off at about $N = 65$. Apparently, a pattern in the yield of multiply charged cluster anions as produced by the present method is observed only in the vicinity of the threshold size of the corresponding charge state. Thus, we concentrate here on the comparison between the theoretical and experimental results for the case of trianionic clusters. These show a close correlation, in particular

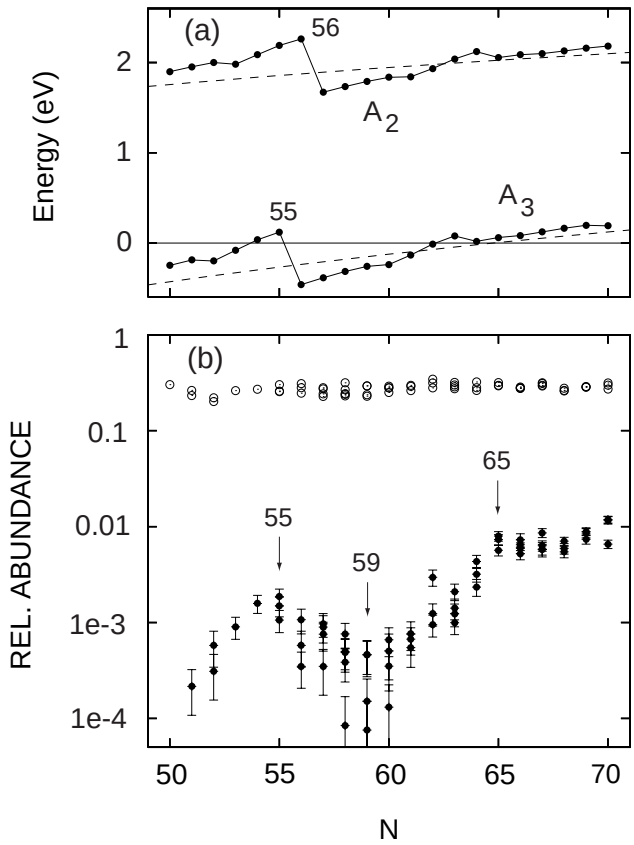

Fig. 1. (a) Calculated second (A_2, upper curve) and third (A_3, lower curve) electron affinities for Au_N clusters at $T = 300$ K in the size range $50 \leq N \leq 70$. Theoretical results from SCM calculations are connected by a solid line, and LDM results [see Eq. (10) with $x = 2$ and 3] are depicted by the dashed lines. (b) Experimental relative abundances of Au_N^{2-} (open circles) and Au_N^{3-} (full circles) as observed after simultaneous storage of Au_N^- and electrons in the Penning trap. (The statistical uncertainties of the individual Au_N^{2-} values are smaller than the symbol size.)

with respect to the general trend and with the presence of the promontory around $N = 55$ in front of the principal branch of the Au_N^{3-} clusters. Comparison of the shell-corrected results (solid dots) with the LDM curve (dashed line) further highlights that electronic shell effects underlie the calculated detailed patterns for A_3 shown in Fig. 1(a) and those observed experimentally in Fig. 1(b).

To explore the energetic stability of the Au_N^{3-} clusters against binary (b) and ternary (t) fission [see Eqs. (1) and (2)], we show in Fig. 2 SCM results for the fission dissociation energies, $\Delta_{N,\gamma}^{3-}$ ($\gamma = b$ or t) associated with the most favorable channel for a given parent Au_N^{3-} cluster. We found that the most favorable channel corresponds to the generation of one or two closed-shell Au^- anions in the case of binary and ternary fission, respectively. Thus $\Delta_{N,b}^{3-} = F(\mathrm{Au}^-) + F(\mathrm{Au}_{N-1}^{2-}) - F(\mathrm{Au}_N^{3-})$ and $\Delta_{N,t}^{3-} = 2F(\mathrm{Au}^-) + F(\mathrm{Au}_{N-2}^-) - F(\mathrm{Au}_N^{3-})$, with the total free energies of the multiply anionic parent and the charged fission products calculated at $T = 300$ K. The fission results

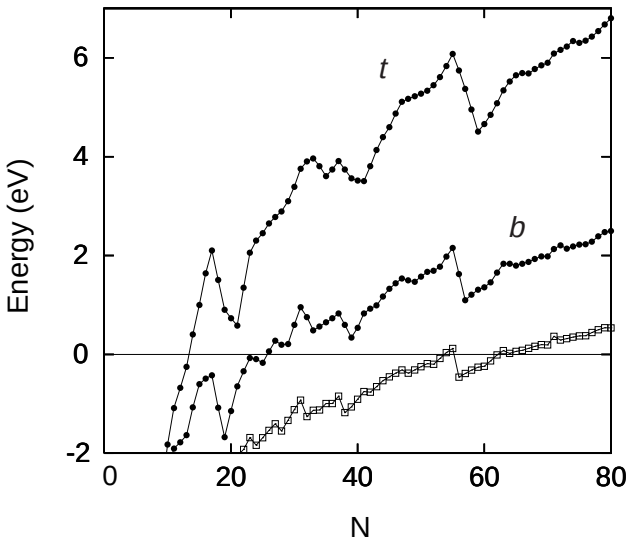

Fig. 2. Theoretical SCM fission dissociation energies (full circles) for the most favorable channel ($\Delta^{3-}_{N,\gamma}$ in eV) at $T = 300$ K for binary ($\gamma = b$, lower curve) and ternary ($\gamma = t$, upper curve) fission of trianionic Au^{3-}_N clusters. For comparison, the theoretical third electron affinities (A_3, open squares) of Au_N clusters at $T = 300$ K are also plotted.

summarized in Fig. 2 for the most favorable channel illustrate that exothermic fission (that is $\Delta^{3-}_{N,\gamma} < 0$) occurs only for the smallest sizes ($N \leq 25$). This, together with the existence of a fission barrier, leads us to conclude that the stability of Au^{3-}_N clusters is dominated by the electron autodetachment process [see Eq. (3)], which is operative when $A_3 < 0$ and involves tunneling through a CB [11], rather than by fission [39].

5 Summary

We studied the generation and stability patterns of the Au^{3-}_N clusters *via* Penning-trap experiments and theoretical SCM investigations and found the following: (i) there is a remarkable agreement between the theoretically predicted and the measured appearance size [$n^{3-}_a(\mathrm{Au}) = 54$]; (ii) the measured yields near the threshold are strongly modulated revealing the influence of electronic shell effects; and (iii) rather than fragmentation *via* fission, we identified electron autodetachment as the prevalent channel governing the clusters' stability. Finding (iii) holds for doubly charged clusters, too [11(b), 13], and leads to appearance sizes unrelated to those known from the more familiar case of multiply charged cationic clusters. It will be of interest to further explore the properties of stored multiply-charged metal cluster anions by either collisional or photo activation [40], as well as to investigate their chemical properties [41].

This research is supported by grants from the U.S. Department of Energy (Grant No. FG05-86ER45234), the Deutsche Forschungsgemeinschaft, the EU networks "EUROTRAPS" and "CLUSTER COOLING", the Materials Science Research Center Mainz and the Fonds der Chemischen Industrie.

References

1. C. Coulomb, *Mémoires de l'Académie* (1786) p. 67ff; *ibid.* (1787) p. 452; M. Faraday, *Experimental research in electricity* (Dover, New York, 1965), Vol. I, p. 360ff.
2. M.A. Kastner, Phys. Today **46**, 24 (1993).
3. S.N. Sauer *et al.*, Phys. Rev. Lett. **65**, 625 (1990); R.L. Hettich *et al.*, Phys. Rev. Lett. **67**, 1242 (1991); P.A. Limbach *et al.*, J. Am. Chem. Soc. **113**, 6795 (1991).
4. C. Yannouleas, U. Landman, Chem. Phys. Lett. **217**, 175 (1994).
5. X.-B. Wang *et al.*, Phys. Rev. Lett. **81**, 3351 (1998).
6. For experimental studies of cationic clusters, see C. Bréchignac *et al.*, Phys. Rev. Lett. **64**, 2893 (1990); *ibid.* **72**, 1636 (1994); Comments At. Mol. Phys. **31**, 361 (1995); T.P. Martin *et al.* Chem. Phys. Lett. **196**, 113 (1992); L. Schweikhard *et al.*, Hyperf. Interact. **99**, 97 (1996); S. Krückeberg *et al.*, Phys. Rev. A **60**, 1251 (1999); U. Näher *et al.*, Phys. Rep. **285**, 245 (1997).
7. R.N. Barnett *et al.*, Phys. Rev. Lett. **67**, 3058 (1991); C. Yannouleas, U. Landman, J. Phys. Chem. **99**, 14577 (1995).
8. For a theoretical review of cationic metal clusters, see C. Yannouleas, U. Landman, R.N. Barnett, in *Metal Clusters*, edited by W. Ekardt (Wiley, New York, 1999), Ch. 4.
9. (a) C. Yannouleas, U. Landman, Phys. Rev. B **51**, 1902 (1995); (b) Phys. Rev. Lett. **78**, 1424 (1997).
10. J.P. Connerade *et al.*, J. Phys. B **32**, 877 (1999); V. Kasperovich *et al.*, Phys. Rev. Lett. **85**, 2729 (2000).
11. (a) C. Yannouleas, U. Landman, Chem. Phys. Lett. **210**, 437 (1993); Phys. Rev. B **48**, 8376 (1993); (b) Phys. Rev. B **61**, R10587 (2000).
12. A. Herlert *et al.*, Phys. Scripta **T80**, 200 (1999).
13. L. Schweikhard *et al.*, Philos. Mag. B **79**, 1343 (1999).
14. A. Herlert *et al.*, Hyperf. Interact. **127**, 529 (2000).
15. C. Stoermer *et al.*, Int. J. Mass Spetrom. **206**, 63 (2001).
16. A. Herlert *et al.*, Eur. Phys. J. D **16**, 65 (2001).
17. C. Yannouleas, U. Landman, A. Herlert, L. Schweikhard, Phys. Rev. Lett. **86**, 2996 (2001).
18. J. Ziegler *et al.*, Hyp. Int. **115**, 171 (1998); J. Ziegler *et al.*, Int. J. Mass Spectrom. **202**, 47 (2000).
19. The relevance of this decay channel for metal clusters was first suggested in the theoretical investigations of Ref. [11(a)], where the appearance sizes of Na^{x-}_N, K^{x-}_N, and Al^{x-}_N ($2 \leq x \leq 4$) were estimated using the LDM expression (10).
20. M.A. Preston, R.K. Bhaduri, *Structure of the Nucleus* (Addison-Wesley, London, 1975).
21. S. Åberg *et al.*, Phys. Rev. C **58**, 3011 (1998).
22. R. Denton *et al.*, Phys. Rev. B **7**, 3589 (1973).
23. R. Kubo, J. Phys. Soc. Jap. **17**, 975 (1962).
24. V.M. Strutinsky, Nucl. Phys. A **95**, 420 (1967).
25. R. Rossignoli, Phys. Rev. C **51**, 1772 (1995).
26. A.S. Jensen, J. Damgaard, Nucl. Phys. A **203**, 578 (1973).
27. *Handbook of Chemistry and Physics*, edited by R.C. Weast (CRC Press, Cleveland, 1974), p. F-23.
28. J. Emsley, *The Elements* (Oxford University Press, New York, 1991).

29. L.D. Landau, E.M. Lifshitz, *Statistical Physics* (Pergamon, Oxford, 1980), Part 1, Ch. XII.
30. D.L. Hill, J.A. Wheeler, Phys. Rev. **89**, 1102 (1953).
31. C. Yannouleas *et al.*, Phys. Rev. B **41**, 6088 (1990); J.M. Pacheco *et al.*, Phys. Rev. Lett. **61**, 294 (1988).
32. Å. Bohr, B.R. Mottelson, *Nuclear Structure* (Benjamin, Reading, MA, 1975), Vol. II.
33. L. Schweikhard *et al.*, Phys. Scripta **T59**, 236 (1995); L. Schweikhard *et al.*, Eur. Phys. J. D **9**, 15 (1999); L. Schweikhard *et al.*, *The Physics and Chemistry of Clusters*, edited by E.E.B. Campbell, M. Larsson, Proceedings of the Nobel Symposium 117 (World Scientific, Singapore, 2001), pp. 267-277.
34. T.G. Dietz *et al.*, J. Chem. Phys. **74**, 6511 (1981); H. Weidele *et al.*, Z. Phys. D **20**, 425 (1991).
35. H. Schnatz *et al.*, Nucl. Instr. Meth. A **251**, 17 (1986).
36. L.S. Brown, G. Gabrielse, Rev. Mod. Phys. **58**, 233 (1986); St. Becker *et al.*, Rev. Sci. Instrum. **66**, 4902 (1995).
37. For the Au_N clusters discussed here ($N \leq 80$), our results at $T = 0$ K and $T = 300$ K differ only slightly. For cases where the SCM reveals significant thermal effects (*i.e.*, for higher temperatures and/or larger r_s's as in the case of Na_N and K_N clusters), see Ref. [9(b)].
38. For Au_N^{x-} clusters, the $T = 0$ parameters entering in the SCM calculation (for definitions see Ref. [9(a)]) are $U_0 = -0.045$, $r_s = 3.01$ a.u., $t = 0.37$ a.u., $\delta_0 = 1.31$ a.u., $\delta_2 = 0$, $W = 5.31$ eV, $\alpha_v = -8.06$ eV, $\alpha_s = 2.52$ eV, and $\alpha_c = 1.04$ eV. For an additional explanation, see footnote 17 in Ref. [9(b)]. The temperature dependence of the surface tension and the coefficient of linear thermal expansion were taken from standard tables.
39. A similar conclusion can be drawn for the case of doubly anionic metal clusters (see Ref. [11(b)]).
40. For such studies of singly charged metal clusters, see S. Krückeberg *et al.*, J. Chem. Phys. **110**, 7216 (1999); U. Hild *et al.*, Phys. Rev. A **57**, 2786 (1998); H. Weidele *et al.*, Eur. Phys. J. D **9**, 173 (1999); J. Chem. Phys. **110**, 8754 (1999).
41. For the effect of the (negative) charge state (with $x \leq 1$) of gold clusters on their chemical reactivity, see D.M. Cox *et al.*, Z. Phys. D **19**, 353 (1991); A. Sanchez *et al.*, J. Phys. Chem. A **103**, 9573 (1999).